

AperTO - Archivio Istituzionale Open Access dell'Università di Torino

## Effector role of cytochrome P450 reductase for androstenedione binding to human aromatase

### This is the author's manuscript

*Original Citation:*

*Availability:*

This version is available <http://hdl.handle.net/2318/1766791> since 2021-01-14T12:42:18Z

*Published version:*

DOI:10.1016/j.ijbiomac.2020.07.163

*Terms of use:*

Open Access

Anyone can freely access the full text of works made available as "Open Access". Works made available under a Creative Commons license can be used according to the terms and conditions of said license. Use of all other works requires consent of the right holder (author or publisher) if not exempted from copyright protection by the applicable law.

(Article begins on next page)

# Effector role of cytochrome P450 reductase for androstenedione binding to human aromatase.

Chao Zhang, Gianluca Catucci, Giovanna Di Nardo\* and Gianfranco Gilardi\*

Department of Life Sciences and Systems Biology, University of Torino, Via Accademia Albertina 13, Torino, 10123, Italy.

\*Co-corresponding authors:

Gianfranco Gilardi

Via Accademia Albertina 13, 10123, Torino, Italy.

Telephone number: +39 011 6704593

Fax number: +39 011 6704643

e-mail: [gianfranco.gilardi@unito.it](mailto:gianfranco.gilardi@unito.it)

Giovanna Di Nardo

Via Accademia Albertina 13, 10123, Torino, Italy.

Telephone number: +39 011 6704689

Fax number: +39 011 6704508

e-mail: [giovanna.dinardo@unito.it](mailto:giovanna.dinardo@unito.it)

## **Abstract**

Cytochromes P450 constitute a large superfamily of monooxygenases involved in many metabolic pathways. Most of them are not self-sufficient and need a reductase protein to provide the electrons necessary for catalysis. It was shown that the redox partner plays a role in the modulation of the structure and function of some bacterial P450 enzymes.

Here, the effect of NADPH-cytochrome reductase (CPR) on human aromatase (Aro) is studied for what concerns its role in substrate binding. Pre-steady-state kinetic experiments indicate that both the substrate binding rates and the percentage of spin shift detected for aromatase are increased when CPR is present. Moreover, aromatase binds the substrate through a conformational selection mechanism, suggesting a possible effector role of CPR. The thermodynamic parameters for the formation of the CPR-Aro complex were studied by isothermal titration calorimetry. The dissociation constant of the complex formation is 4.5 folds lower for substrate-free compared to the substrate-bound enzyme. The enthalpy change observed when the CPR-Aro complex forms in the absence of the substrate are higher than in its presence, indicating that more interactions are formed/broken in the former case.

Taken together, our data confirm that CPR has a role in promoting aromatase conformation optimal for substrate binding.

## **Keywords**

Aromatase, cytochrome P450 reductase, isothermal titration calorimetry.

## 1. Introduction

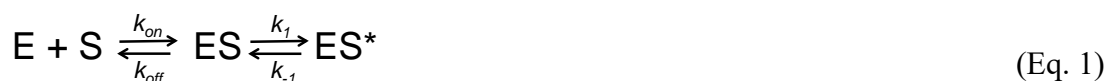
Human cytochromes P450 (P450) are membrane-bound proteins present in most tissues of the human body [1]. They play essential roles in the metabolism of steroid hormones, vitamins and fatty acids and they also can oxidize xenobiotics such as carcinogens and drugs. They are not self-sufficient enzymes and most of them share the reduction partner, cytochrome P450 reductase (CPR). Electrons from NADPH are stepwise transferred from CPR to the P450 heme group and protein-protein interaction has been demonstrated to be guided mainly by electrostatic interactions with the positively charged heme-proximal side of the P450 enzyme and the negatively charged residues on FMN-binding domain of CPR [2–4] as well as by hydrophobic interactions [5]. CPR and cytochromes P450 are anchored to the membrane through their hydrophobic N-terminal transmembrane helices. The anchoring of the proteins in the lipid bilayer was shown to play an important role due to the influence of both the lipid environment and the membrane-anchor helices on electron transfer and P450 catalytic efficiency [6-7]. Solid-state NMR studies in membrane-mimicking environments such as lipid nanodiscs have shown that protein-lipid interaction are crucial for the stability, the dynamics and the interaction between human cytochromes P450 and the redox partners CPR [8-12] and cytochrome b<sub>5</sub> [13-15]. Moreover it was shown that CPR and cytochrome b<sub>5</sub> compete for cytochromes P450 binding and that the presence of the substrate affects the interplay between the three proteins promoting the binding of cytochrome b<sub>5</sub> to the P450 enzyme [15].

In addition to electron transfer, different studies have shown that the redox partners can play important roles in regulating the structure and function of some bacterial P450 enzymes [16-20]. As a consequence, the topic of the interaction between cytochromes P450 and its redox partner is attracting more and more attention and an important question is whether CPR plays a role in modulating the structure and function of human P450s.

Here we investigate the role played by CPR in modulating the substrate binding

ability of human aromatase. This enzyme is involved in the estrogens synthesis and it catalyzes the conversion of androgens to estrogens via a three-step reaction [21–23]. Due to its important role in breast cancer development and progression [24,25], the structure-function relationship of aromatase has been widely studied [26–32]. This enzyme is highly selective for the androgen substrates with  $K_M$  values reported in the low  $\mu\text{M}$ - $\text{nM}$  range [30,33] and it also shows a high coupling efficiency (87%) [34], when compared to other human more promiscuous cytochromes P450, indicating an optimal interaction with CPR.

Many cytochromes P450 have been shown to adopt different conformations ranging from the open form, typical of the ligand free-enzymes, to the closed one that is adopted when a substrate or inhibitor is present [35]. The crystal structure of aromatase is available only in complex with the substrate androstenedione. The protein is in a closed conformation and the substrate is perfectly accommodated in a relatively small active site [26,28,36]. This implies that aromatase needs to undergo structural changes to make the active site accessible to the substrate [27,37,38]. Indeed, FTIR and time-resolved fluorescence spectroscopy studies revealed that in the absence of substrate, the flexibility of aromatase increases with faster dynamics of helix F involved in the substrate access channel [36,39]. Thus, it has been hypothesized that aromatase adopts different conformations according to the presence and absence of the substrate. In general, the study of how the conformational dynamics of cytochromes P450 are associated with ligand binding events is another important topic in the research field. Recently, it has been shown that many human P450 enzymes use a conformational selection mechanism rather than an induced fit one [40,41]. In the induced fit model, the substrate (S) binds to the enzyme (E) and causes a conformational change in the protein to give the optimal ligand-bound conformation, indicated as  $\text{ES}^*$  in Equation 1 (Scheme 1A):



In the conformational selection model, the substrate (S) binds one of the possible conformations of the enzyme that is the one optimal for substrate binding, indicated by E\* in Equation 2 (Scheme 1B):



In the present study, a combination of substrate titrations followed spectrophotometrically, as well as pre-steady state kinetics of substrate binding and isothermal titration calorimetry are used to gain information on the effect of CPR on human aromatase (Aro) ability to bind the substrate and on the thermodynamics of CPR-Aro complex formation. The presence of CPR is found to increase the rates for substrate binding and to increase the number of molecules that are in the optimal conformation to bind the substrate. The results support that Aro binds the substrate through a conformational selection mechanism with the CPR having a higher affinity when the substrate is not present in the active site of the protein.

## 2. Materials and methods

### 2.1 Chemicals

All solvents and reagents were of analytical grade and were obtained from Sigma Aldrich.

### 2.2 Protein expression and purification

The recombinant form of human aromatase used in this work lacks the N-terminal amino acid fragment anchoring the protein to the membrane (residues 1-39) that was replaced by 10 residues (MAKKTSSKGR). Moreover, a four-histidine tag was introduced at the C-terminal [39]. The recombinant protein was expressed and

purified as described previously [39]. Briefly, transformed *Escherichia coli* DH5 $\alpha$  cells were grown at 37 °C in a Terrific Broth media until the cell density OD<sub>600</sub> reached 0.6. Protein expression was induced with 1 mM isopropyl- $\beta$ -D-thiogalactopyranoside and carried out at 28 °C for 48 hours. The cells were then harvested and resuspended in 100 mM potassium phosphate (KPi) pH 7.4, 20% glycerol, 1 mM  $\beta$ -mercaptoethanol, 0.1% v/v Tween-20 buffer containing 1 mg/mL lysozyme, 1% v/v Tween-20 and protease inhibitor mixture. After stirring for 45 minutes, cells were disrupted by sonication and ultra-centrifuged at 40,000 rpm for 25 min at 4 °C. The supernatant was first loaded onto a diethyl aminoethyl (DEAE) ion-exchange chromatography and then further purified by a Nickel-ion affinity chromatography. The target protein was eluted with a linear gradient in which histidine ranging from 10 to 40 mM was added. The eluted fractions were pooled according to the purity ratio ( $A_{280nm}/A_{418nm}$ ) and concentrated by Amicon centrifugal filters (30 kDa MWCO membrane). Aro concentration was estimated by CO-binding assay, using an extinction coefficient at 450 nm of 91,000 M<sup>-1</sup> cm<sup>-1</sup> [42].

Human CPR was expressed as a full-length protein in *Escherichia coli* DH5 $\alpha$ . The cells were resuspended in a 100 mM Tris-acetate buffer, pH 7.6, 0.5 M sucrose and 1 mM EDTA buffer and lysed by adding with 0.5 mg/mL lysozyme and 0.1 mM EDTA for 30 min at 4°C. After centrifugation at 4,000 rpm for 20 min, the pellets were resuspended in 100 mM KPi, pH 7.6, 6 mM magnesium acetate, 0.1 mM DTT, 20% glycerol, 0.2 mM PMSF and 0.1 mM DNase I, and disrupted by sonication. The membrane-containing pellets were collected by 40 min centrifugation at 40,000 rpm, suspended in 20 mM KPi, pH 7.6, 20% glycerol, 0.1 mM EDTA, 0.2 mM PMSF, 0.2 % sodium cholate and 0.2 % Triton X-100, and stirred gently for 2 h. This crude extract was then centrifugated at 40,000 rpm for 1h, and the supernatant was load onto a pre-equilibrated affinity chromatography of 2',5'-ADP Sepharose 4B. After different washing steps with the equilibration buffer, where first 250 mM NaCl and then 2 mM adenosine were added, the CPR was eluted with a linear gradient in which NADP<sup>+</sup> increased from 0.1 to 1 mM. Fractions containing the full-length CPR, which were

monitored by SDS-PAGE analysis, were pooled and concentrated by Amicon centrifugal filters (with 30 kDa MWCO membrane). The CPR concentrations were measured using an extinction coefficient at 456 nm of 24,100 M<sup>-1</sup> cm<sup>-1</sup> [43].

### 2.3 UV-vis spectroscopy and substrate binding titrations

Spectral binding titrations were performed as described previously [30]. In brief, 1  $\mu$ M of aromatase in 100 mM KPi buffer pH 7.0, 20% glycerol, 1 mM  $\beta$ -mercaptoethanol were incubated with increasing amounts of androstenedione ranging from 0.5  $\mu$ M to 12  $\mu$ M. Binding assay was using an Agilent 8453 UV-vis spectrophotometer at 25 °C. UV-visible spectra were recorded after each addition, and the absorbance differences at 394 nm and at 418 nm were plotted against the added substrate concentrations. The data were fitted to the following equation that allowed to calculate the dissociation constants  $K_D$ :

$$\Delta A_{394-418} = \Delta A^{\max}_{394-418} \cdot [S]_{\text{free}} / (K_D + [S]_{\text{free}})$$

where  $[S]_{\text{free}}$  is  $[S]_{\text{total}} - [E \cdot S]$  and  $[E \cdot S] = \Delta A_{394-418} [E]_{\text{total}} / \Delta A^{\max}_{394-418}$ .

### 2.4 Stopped flow absorbance experiments

The pre-steady state kinetics of substrate binding to aromatase was investigated using a Hi-Tech scientific SF-61 single mixing stopped-flow instrument (TgK Scientific, UK). In a typical experiment, one of the drive syringes contained the purified aromatase (2  $\mu$ M) in a 100 mM potassium phosphate buffer pH 7.0 containing 10% glycerol, 1 mM  $\beta$ -mercaptoethanol. The second drive syringe contained different concentrations of the substrate androstenedione. For the experiments in the presence of CPR, the purified protein (6  $\mu$ M) was pre-incubated with aromatase in the first drive syringe and then mixed with the substrate androstenedione.

In all the experiments, the temperature was set at 25 °C and controlled by a water bath.



For each substrate concentration, 5 to 7 replicates were conducted for each experiment. Each Kinetic trace was derived from observing the changes at 394 nm as a function of time and fitted to a single or double exponential function by Kinetic studio V3 software (TgK Scientific, UK).

## **2.5 Isothermal titration calorimetry**

Isothermal titration calorimetry (ITC) experiments were performed at 25°C using a MicroCal iTC200 instrument (Malvern Instruments, Malvern, UK). Before the experiment, aromatase and CPR were prepared by extensive buffer-exchange using Amicon centrifugal filters (30 kDa MWCO) and concentrated with the same potassium phosphate buffer (100 mM KPi, 10% glycerol, pH 7.0). For the experiments in the presence of the substrate, aromatase (0.5  $\mu$ M) was incubated overnight at 4°C with saturating amounts of the substrate androstenedione (20  $\mu$ M). The reaction cell was filled with 300  $\mu$ L of 25  $\mu$ M aromatase and the injection syringe was filled with 600  $\mu$ M CPR. CPR was titrated into Aro in potassium phosphate buffer (100 mM KPi, 10% glycerol, pH 7.0) up to a 1:5 (Aro:CPR) molar ratio. The first injection was 0.1  $\mu$ L with 0.2 s duration and omitted during data analysis. The second injection was 3.5  $\mu$ L with 7 s duration followed by 9 injections of 4  $\mu$ L with 8 s duration. Each titration experiment involved a 90 s interval between injections. The reaction cell was continuously stirred at 750 rpm speed. A reference power of 7 was used for each experiment. The data were processed and analyzed by using Origin<sup>®</sup> 7.0 software. Control experiments were carried out by titrating the ligand CPR into the cell containing only the buffer under identical conditions. The heats of dilution were subtracted from the observed titration data.

## **3. Results and Discussion**

### **3.1 Effect of CPR on substrate binding by aromatase.**

The effect of CPR on the affinity ( $K_D$ ) of human aromatase toward its substrate was first investigated by UV-vis spectroscopy. In general, the binding of the substrate in the active site of cytochromes P450 is known to alter the spin state of the heme iron, with a spectral transition that for aromatase occurs from 418 to 394 nm [39]. Here the substrate binding curves values were obtained by monitoring the spin shift caused by the addition of increasing concentrations of androstenedione to 1  $\mu$ M of Aro and data were fitted to one-site saturation binding curves, from which an apparent  $K_D$  of  $0.98 \pm 0.11$   $\mu$ M and  $0.72 \pm 0.11$   $\mu$ M were found in the absence and in the presence 3-fold excess of CPR, respectively. These results are not significantly different and indicate that CPR does not affect the binding affinity of Aro for the substrate androstenedione.

Pre-steady state kinetics of substrate binding were then investigated by stopped-flow measurements in the absence and presence of CPR. First, different concentrations of the substrate (0.25-30  $\mu$ M) were used with a fixed concentration of Aro (1  $\mu$ M) in the absence and presence of 3  $\mu$ M of CPR. Figure 1 shows the difference spectra obtained with the typical low-to-high spin transition due to substrate binding. When the percentage of spin shift obtained at different substrate concentrations was measured, the data showed consistent lower values in the absence of CPR (Figure 2). In particular, at the lowest substrate concentration used (0.25-0.5  $\mu$ M), the spin shift obtained in the absence of CPR was 40% lower than that obtained in its presence (Figure 2). These data indicate that CPR increases the population of Aro that binds the substrate, suggesting a possible regulatory role on the conformation on the P450 enzyme, as previously reported for P450cam [20].

The kinetics of substrate binding were followed as the increase of the signal at 394 nm in the first 3 seconds and the traces obtained were found to better fit to a single exponential function from which the rate constants were derived (Figure 3). The plot of the rates as a function of substrate concentration shows a linear trend both in the absence and presence of CPR (Figure 4A). However, the substrate binding rates were increased by up to 30% when saturating amounts of the substrate were tested (Figure 4A). A linear regression was applied to calculate the apparent second-order rate

constants ( $k_{\text{on}}$  and  $k_{\text{off}}$ ). In the absence of CPR, the obtained  $k_{\text{on}}$  value was  $5.1 \times 10^5 \text{ M}^{-1} \text{ s}^{-1}$  and the  $k_{\text{off}}$  was  $0.17 \text{ s}^{-1}$  (Table 1). However, both the apparent  $k_{\text{on}}$  and  $k_{\text{off}}$  were increased when an excessive CPR was added. The calculated  $k_{\text{on}}$  and  $k_{\text{off}}$  were  $7.0 \times 10^5 \text{ M}^{-1} \text{ s}^{-1}$  and was  $0.24 \text{ s}^{-1}$ , respectively.  $K_D$  values calculated from these kinetic constants ( $k_{\text{off}}/k_{\text{on}}$ ) are in the same order of magnitude with the  $K_D$  values measured by spectroscopic titrations (Table 1).

One of the interesting questions in the cytochrome P450 research field is whether they bind their substrates/inhibitors through conformational selection modes or induced fit. When an increasing hyperbolic dependence of the binding rates ( $k_{\text{obs}}$ ) as a function of substrate concentration is found, this is diagnostic of an induced fit mechanism [44]. On the other hand, a decreasing dependence in the binding rates ( $k_{\text{obs}}$ ) as a function of substrate concentration is diagnostic of conformational selection [44,45]. However, conformational selection can give rise to increasing trends as well. In this case, a possible way to distinguish between the two modes is to carry out two separate experiments. In a first experiment, the concentration of the enzyme is fixed and the one of the substrate is varied; in a second experiment, the concentration of the substrate is fixed and the one of the enzyme is varied. When the plots of the  $k_{\text{obs}}$  obtained in the two experiments are constructed, the same trend should be found in the case of an induced fit mechanism whereas distinct kinetics are found in the case of the conformation selection mode [44].

In the case of Aro, the plot of the rates as a function of androstenedione concentration (Figure 4A) shows a linear trend. This suggests a conformational selection mode as an induced fit should have a hyperbolic dependence [44]. To gain further information, a second set of experiments was carried out keeping the substrate concentration fixed at  $2 \mu\text{M}$  while varying the enzyme concentration. The plots obtained (Figure 4B) show a non-linear dependence. The two plots where either the protein or the ligand are varied should be identical in the case of an induced fit mechanism [44], therefore it can be concluded that a conformational selection mode is taking place in substrate binding by aromatase.

Taken together, the data show that the presence of CPR does not cause any change in the substrate binding affinity of aromatase, but it increases the binding rate for the substrate as well as the fraction of the enzyme that is able to bind the substrate through a conformational selection mechanism. This is consistent with Equation 2, Scheme 1B.

### 3.2 Isothermal Titration Calorimetry (ITC)

The thermodynamic characterization of a binding process is traditionally investigated by isothermal titration calorimetry (ITC). Therefore the binding process of CPR to aromatase in the absence and presence of the substrate androstenedione was followed by ITC. One important issue about this experiment is the reduction state of CPR. Indeed, it is known that the semiquinone state of CPR (CPR<sub>sq</sub>) has the highest affinity for other human P450s as demonstrated for P450 2C9 [46]. Upon reduction, the fully oxidized CPR (CPR<sub>ox</sub>) undergoes the conformational changes required for the CPR<sub>sq</sub> to be able to dock the P450 proximal side. This forms a complex where the FMN of the CPR<sub>sq</sub> and then heme of the P450 are close enough to allow electron transfer [47,48].

For these reasons, the UV-vis spectra of the CPR and the Aro used in the ITC experiments were collected to confirm the oxidation state of the two proteins (Figure 5). In particular, the spectrum of CPR in Figure 5A shows a band at 587 nm with a shoulder at 630 nm, typical of the its semiquinone state (CPR<sub>sq</sub>). This confirms that CPR is purified in its semiquinone state as previously reported [49,50]. Figure 5B shows the spectra recorded of Aro in the absence and presence of the substrate androstenedione. The presence of bands at 418 and 394 nm indicate that the protein undergoes the typical low-to-high spin state changes upon substrate binding.

We therefore proceeded to collect the ITC profiles resulting from the titration of CPR<sub>sq</sub> into the cell containing Aro in experiments carried out both in the presence and absence of androstenedione (Figure 6). The titration was carried out in a 100 mM KPi

pH 7.0 buffer containing 10% glycerol and the final CPR<sub>sq</sub> : Aro molar ratio achieved was 5:1. In all cases the ITC profiles show the presence of an exothermic followed by an endothermic process. These profiles are not present in control experiments where the CPR<sub>sq</sub> was titrated in a solution containing only buffer. Moreover, when the heat of the endothermic and the exothermic processes are plotted as a function of the CPR<sub>sq</sub>: Aro molar ratio, a sigmoidal trend typical of ligand binding is obtained with the endothermic process contributing more to the overall process (data not shown). Thus, the two processes can be assigned to the CPR<sub>sq</sub>-Aro complex formation. The thermodynamic parameters were obtained by fitting the overall data (Figure 6) and they are reported in Table 2. In the absence of the substrate, the interaction between Aro and CPR<sub>sq</sub> yielded a  $K_D$  value of  $5.4 \pm 1.2 \mu\text{M}$ , while in the presence of the substrate the  $K_D$  was  $24.2 \pm 6.9 \mu\text{M}$ . These results suggested that CPR<sub>sq</sub> binds to the substrate-free Aro with a higher affinity compared to the substrate-bound form. Interestingly, the enthalpy changes of the interaction between CPR<sub>sq</sub> and Aro are also significantly altered by the presence of the substrate. In fact, these are considerably higher than when the substrate is not present, indicating that more interactions are forming and breaking when substrate-free Aro complexes with CPR<sub>sq</sub>. This finding also suggests that more conformational changes are taking place in CPR<sub>sq</sub> and aromatase when the substrate is not present.

The overall  $\Delta G$  resulted negative as well as  $-T\Delta S$  indicating that the binding is entropically driven. This finding suggests a large entropic contribution that can be due to the release or replacement of ordered water molecules from the protein surface and to the proteins' conformational dynamics during complex formation [51]. The positive  $\Delta H$  values suggest that the binding of CPR<sub>sq</sub> to aromatase is composed of intramolecular hydrogen bonding and non-covalent interaction following conformational changes of CPR<sub>sq</sub>. It has to be taken into account that ITC experiments were carried out under a single buffer condition known to maintain protein stability and solubility. Moreover, the proteins are not in their physiological membrane environment that is known to affect and limit their orientation promoting

complex formation also through the transmembrane helix [14]. However, the thermodynamic parameters calculated by ITC are in line with those recently calculated by surface plasmon resonance (SPR) for the interaction of CPR<sub>sq</sub> with many human cytochromes P450, including aromatase [52]. Also in that case, the process resulted entropically driven with a positive value of  $\Delta H$  [52].

#### **4. Conclusion**

In conclusion, this study provides new insights on the interaction of a human cytochrome P450 with the redox partner, indicating an effector role of CPR, as previously observed for bacterial cytochrome P450cam [19,20].

Here we show not only that human Aro adopts the conformational selection mode to bind the substrate, but also that CPR when bound to substrate-free Aro triggers the conformational changes required for optimal substrate binding (Scheme 1B). These data are consistent with the recent results coming from all-atom molecular dynamics simulations showing that CPR binding alters the motions of human aromatase and reshapes the substrate access channel [53].

The effector role of CPR can be crucial in the physiological environment since the reductase protein is in limited amounts compared to cytochromes P450 [54] and would therefore promote catalysis when already in the semi-reduced form and ready to bind the enzyme. It would be interesting to expand this kind of studies to other human enzymes, such as the more promiscuous cytochromes P450 involved in drug metabolism, to highlight possible preferences of CPR for the different enzymes according to their physiological role in the organism.

## **Acknowledgements**

CZ thanks China Scholarship Council (CSC) for financial support.

## **Author contributions**

CZ, GG, GDN and GG designed the experiments; CZ and GC performed the experiments; CZ, GC, GDN and GG analyzed the data; CZ and GDN wrote the paper. All authors reviewed and approved this article.

## **Conflicts of interest**

The authors declare that there is no conflict of interest.

## References

- [1] S.D. Black, Membrane topology of the mammalian P450 cytochromes, *FASEB J.* 6 (1992) 680–685. <https://doi.org/10.1096/fasebj.6.2.1537456>.
- [2] M. Wang, D.L. Roberts, R. Paschke, T.M. Shea, B.S.S. Masters, J.J. Kim, Three-dimensional structure of NADPH–cytochrome P450 reductase: prototype for FMN- and FAD-containing enzymes, *Proc. Natl. Acad. Sci USA.* 94 (1997) 8411–8416. <https://doi.org/10.1073/pnas.94.16.8411>.
- [3] Y. Hong, R. Rashid, S. Chen, Binding features of steroidal and nonsteroidal inhibitors, *Steroids.* 76 (2011) 802–806. <https://doi.org/10.1016/j.steroids.2011.02.037>.
- [4] Y. Hong, H. Li, Y.C. Yuan, S. Chen, Sequence–function correlation of aromatase and its interaction with reductase, *J. Steroid Biochem. Mol. Biol.* 118 (2010) 203–206. <https://doi.org/10.1016/j.jsbmb.2009.11.010>.
- [5] C. Kenaan, H. Zhang, E.V. Shea, P.F. Hollenberg, Uncovering the role of hydrophobic residues in cytochrome P450–cytochrome P450 reductase interactions, *Biochemistry.* 50 (2011) 3957–3967. <https://doi.org/10.1021/bi1020748>.
- [6] P. Hlavica, Mechanistic basis of electron transfer to cytochromes P450 by natural redox partners and artificial donor constructs, *Adv. Exp. Med. Biol.* 851 (2015) 247–297. [https://doi.org/10.1007/978-3-319-16009-2\\_10](https://doi.org/10.1007/978-3-319-16009-2_10).
- [7] U.H.N. Dürr, L. Waskell, A. Ramamoorthy, The cytochromes P450 and b5 and their reductases-promising targets for structural studies by advanced solid-state NMR spectroscopy, *Biochim. Biophys. Acta-Biomembr.* 1768 (2007) 3235–3259. <https://doi.org/10.1016/j.bbamem.2007.08.007>.
- [8] C. Barnaba, K. Gentry, N. Sumangala, A. Ramamoorthy, The catalytic function of cytochrome P450 is entwined with its membrane-bound nature, *F1000Res.* 6 (2017) 662. <https://doi.org/10.12688/f1000research.11015.1>.
- [9] C. Barnaba, A. Ramamoorthy, Picturing the membrane-assisted choreography



- of cytochrome P450 with lipid nanodiscs, *ChemPhysChem*. 19 (2018) 2603–2613. <https://doi.org/10.1002/cphc.201800444>.
- [10] C. Barnaba, T. Ravula, I.G. Medina-Meza, S.C. Im, G.M. Anantharamaiah, L. Waskell, A. Ramamoorthy, Lipid-exchange in nanodiscs discloses membrane boundaries of cytochrome-P450 reductase, *Chem. Commun.* 54 (2018) 6336–6339. <https://doi.org/10.1039/C8CC02003E>.
- [11] E. Prade, M. Mahajan, S.C. Im, M. Zhang, K.A. Gentry, G.M. Anantharamaiah, L. Waskell, A. Ramamoorthy, A minimal functional complex of cytochrome P450 and FBD of cytochrome P450 reductase in nanodiscs, *Angew. Chem. Int. Ed.* 57 (2018) 8458–8462. <https://doi.org/10.1002/anie.201802210>.
- [12] M. Mahajan, T. Ravula, E. Prade, G.M. Anantharamaiah, A. Ramamoorthy, Probing membrane enhanced protein-protein interactions in a minimal redox complex of cytochrome-P450 and P450-reductase, *Chem. Commun.* 55 (2019) 5777–5780. <https://doi.org/10.1039/C9CC01630A>.
- [13] S. Ahuja, N. Jahr, S.C. Im, S. Vivekanandan, N. Popovych, S.V. Le Clair, R. Huang, R. Soong, J. Xu, K. Yamamoto, R.P. Nanga, A. Bridges, L. Waskell, A. Ramamoorthy, A Model of the Membrane-bound Cytochrome b5-Cytochrome P450 Complex from NMR and Mutagenesis Data, *J. Biol. Chem.* 288 (2013) 22080–22095. <https://doi.org/10.1074/jbc.M112.448225>.
- [14] K. Yamamoto, M.A. Caporini, S.C. Im, L. Waskell, A. Ramamoorthy, Transmembrane interactions of full-length mammalian bitopic cytochrome-P450-cytochrome-b5 complex in lipid bilayers revealed by sensitivity-enhanced dynamic nuclear polarization solid-state NMR spectroscopy, *Sci. Rep.* 7 (2017) 4116. <https://doi.org/10.1038/s41598-017-04219-1>.
- [15] K.A. Gentry, G.M. Anantharamaiah, A. Ramamoorthy, Probing protein-protein and protein-substrate interactions in the dynamic membrane-associated ternary complex of cytochromes P450, b5, and reductase, *Chem. Commun.* 55 (2019)

- 13422–13425. <https://doi.org/10.1039/C9CC05904K>.
- [16] P.J. Bakkes, J.L. Riehm, T. Sagadin, A. Rühlmann, P. Schubert, S. Biemann, M. Girhard, M.C. Hutter, R. Bernhardt, V.B. Urlacher, Engineering of versatile redox partner fusions that support monooxygenase activity of functionally diverse cytochrome P450s, *Sci. Rep.* 7 (2017) 9570. <https://doi.org/10.1038/s41598-017-10075-w>.
- [17] W. Zhang, Y. Liu, J. Yan, S. Cao, F. Bai, Y. Yang, S. Huang, L. Yao, Y. Anzai, F. Kato, L.M. Podust, D.H. Sherman, S. Li, New reactions and products resulting from alternative interactions between the P450 enzyme and redox partners, *J. Am. Chem. Soc.* 136 (2014) 3640–3646. <https://doi.org/10.1021/ja4130302>.
- [18] T. Sagadin, J.L. Riehm, M. Milhim, M.C. Hutter, R. Bernhardt, Binding modes of CYP106A2 redox partners determine differences in progesterone hydroxylation product patterns, *Commun. Biol.* 1 (2018) 99. <https://doi.org/10.1038/s42003-018-0104-9>.
- [19] S. Tripathi, H. Li, T.L. Poulos, Structural basis for effector control and redox partner recognition in cytochrome P450, *Science*. 340 (2013) 1227–1230. <https://doi.org/10.1126/science.1235797>.
- [20] S.A. Hollingsworth, D. Batabyal, B.D. Nguyen, T.L. Poulos, Conformational selectivity in cytochrome P450 redox partner interactions, *Proc. Natl. Acad. Sci.* 113 (2016) 8723–8728. <https://doi.org/10.1073/pnas.1606474113>.
- [21] E.A. Thompson, P.K. Siiteri, The involvement of human placental microsomal cytochrome P-450 in aromatization, *J. Biol. Chem.* 249 (1974) 5373–5378.
- [22] E.A. Thompson, P.K. Siiteri, Utilization of oxygen and reduced nicotinamide adenine dinucleotide phosphate by human placental microsomes during aromatization of androstenedione, *J. Biol. Chem.* 249 (1974) 5364–5372.
- [23] E.R. Simpson, M.S. Mahendroo, G.D. Means, M.W. Kilgore, M.M. Hinshelwood, S. Graham-Lorence, B. Amarneh, Y. Ito, C.R. Fisher, M.D. Michael, C.R. Mendelson, S.E. Bulun, Aromatase cytochrome P450, the

- enzyme responsible for estrogen biosynthesis, *Endocr. Rev.* 15 (1994) 342–355. <https://doi.org/10.1210/edrv-15-3-342>.
- [24] A. Brodie, G. Sabnis, D. Jelovac, Aromatase and breast cancer, *J. Steroid Biochem. Mol. Biol.* 102 (2006) 97–102. <https://doi.org/10.1016/j.jsbmb.2006.09.002>.
- [25] R.J. Santen, H. Brodie, E.R. Simpson, P.K. Siiteri, A. Brodie, History of aromatase: saga of an important biological mediator and therapeutic target, *Endocr. Rev.* 30 (2009) 343–375. <https://doi.org/10.1210/er.2008-0016>.
- [26] D. Ghosh, J. Griswold, M. Erman, W. Pangborn, Structural basis for androgen specificity and oestrogen synthesis in human aromatase, *Nature*. 457 (2009) 219–223. <https://doi.org/10.1038/nature07614>.
- [27] D. Ghosh, J. Lo, D. Morton, D. Valette, J. Xi, J. Griswold, S. Hubbell, C. Egbuta, W. Jiang, J. An, H.M.L. Davies, Novel aromatase inhibitors by structure-guided design, *J. Med. Chem.* 55 (2012) 8464–8476. <https://doi.org/10.1021/jm300930n>.
- [28] J. Lo, G. Di Nardo, J. Griswold, C. Egbuta, W. Jiang, G. Gilardi, D. Ghosh, Structural basis for the functional roles of critical residues in human cytochrome P450 aromatase, *Biochemistry*. 52 (2013) 5821–5829. <https://doi.org/10.1021/bi400669h>.
- [29] G. Di Nardo, G. Gilardi, Human aromatase: Perspectives in biochemistry and biotechnology, *Biotechnol. Appl. Biochem.* 60 (2013) 92–101. <https://doi.org/10.1002/bab.1088>.
- [30] G. Di Nardo, M. Breitner, A. Bandino, D. Ghosh, G.K. Jennings, J.C. Hackett, G. Gilardi, Evidence for an elevated aspartate pKa in the active site of human aromatase, *J. Biol. Chem.* 290 (2015) 1186–1196. <https://doi.org/10.1074/jbc.M114.595108>.
- [31] R. Baravalle, G. Di Nardo, A. Bandino, I. Barone, S. Catalano, S. Andò, G. Gilardi, Impact of R264C and R264H polymorphisms in human aromatase function, *J. Steroid Biochem. Mol. Biol.* 167 (2017) 23–32.

<https://doi.org/10.1016/j.jsbmb.2016.09.022>.

- [32] D. Ghosh, C. Egbuta, J. Lo, Testosterone complex and non-steroidal ligands of human aromatase, *J. Steroid Biochem. Mol. Biol.* 181 (2018) 11–19. <https://doi.org/10.1016/j.jsbmb.2018.02.009>.
- [33] C.D. Sohl, F.P. Guengerich, Kinetic Analysis of the three-step steroid aromatase reaction of human cytochrome P450 19A1, *J. Biol. Chem.* 285 (2010) 17734–17743. <https://doi.org/10.1074/jbc.M110.123711>.
- [34] R. Baravalle, A. Ciaramella, F. Baj, G. Di Nardo, G. Gilardi, Identification of endocrine disrupting chemicals acting on human aromatase, *Biochim. Biophys. Acta BBA-Proteins Proteomics.* 1866 (2018) 88–96. <https://doi.org/10.1016/j.bbapap.2017.05.013>.
- [35] X. Yu, V. Cojocaru, R.C. Wade, Conformational diversity and ligand tunnels of mammalian cytochrome P450s, *Biotechnol. Appl. Biochem.* 60 (2013) 134–145. <https://doi.org/10.1002/bab.1074>.
- [36] W. Jiang, D. Ghosh, Motion and flexibility in human cytochrome P450 aromatase, *PLoS ONE.* 7 (2012) e32565. <https://doi.org/10.1371/journal.pone.0032565>.
- [37] A. Magistrato, J. Sgrignani, R. Krause, A. Cavalli, Single or multiple access channels to the CYP450s active site? An answer from free energy simulations of the human aromatase enzyme, *J. Phys. Chem. Lett.* 8 (2017) 2036–2042. <https://doi.org/10.1021/acs.jpclett.7b00697>.
- [38] G. Di Nardo, G. Camicata, R. Baravalle, V. Dell’Angelo, A. Ciaramella, G. Catucci, P. Ugliengo, G. Gilardi, Working at the membrane interface: Ligand-induced changes in dynamic conformation and oligomeric structure in human aromatase, *Biotechnol. Appl. Biochem.* 65 (2018) 46–53. <https://doi.org/10.1002/bab.1613>.
- [39] G. Di Nardo, M. Breitner, S.J. Sadeghi, S. Castrignanò, G. Mei, A. Di Venere, E. Nicolai, P. Allegra, G. Gilardi, Dynamics and flexibility of human aromatase probed by FTIR and time resolved fluorescence spectroscopy, *PLoS*

- ONE. 8 (2013) e82118. <https://doi.org/10.1371/journal.pone.0082118>.
- [40] F.P. Guengerich, C.J. Wilkey, T.T.N. Phan, Human cytochrome P450 enzymes bind drugs and other substrates mainly through conformational-selection modes, *J. Biol. Chem.* 294 (2019) 10928–10941. <https://doi.org/10.1074/jbc.RA119.009305>.
- [41] F.P. Guengerich, C.J. Wilkey, S.M. Glass, M.J. Reddish, Conformational selection dominates binding of steroids to human cytochrome P450 17A1, *J. Biol. Chem.* 294 (2019) 10028–10041. <https://doi.org/10.1074/jbc.RA119.008860>.
- [42] T. Omura, R. Sato, The Carbon monoxide-binding pigment of liver microsomes: I. Evidence for its hemoprotein nature, *J. Biol. Chem.* 239 (1964) 2370–2378.
- [43] T.D. Porter, T.E. Wilson, C.B. Kasper, Expression of a functional 78,000 dalton mammalian flavoprotein, NADPH-cytochrome P-450 oxidoreductase, in *Escherichia coli*, *Arch. of Biochem. Biophys.* 252 (1987) 353–367. [https://doi.org/10.1016/0003-9861\(87\)90111-1](https://doi.org/10.1016/0003-9861(87)90111-1).
- [44] S. Gianni, J. Dogan, P. Jemth, Distinguishing induced fit from conformational selection, *Biophys. Chem.* 189 (2014) 33–39. <https://doi.org/10.1016/j.bpc.2014.03.003>.
- [45] A.D. Vogt, E. Di Cera, Conformational selection or induced fit? A critical appraisal of the kinetic mechanism, *Biochemistry.* 51 (2012) 5894–5902. <https://doi.org/10.1021/bi3006913>.
- [46] C. Barnaba, E. Taylor, J.A. Brozik, Dissociation constants of cytochrome P450 2C9/cytochrome P450 reductase complexes in a lipid bilayer membrane depend on NADPH: a single-protein tracking study, *J. Am. Chem. Soc.* 139 (2017) 17923–17934. <https://doi.org/10.1021/jacs.7b08750>.
- [47] C. Barnaba, M.J. Martinez, E. Taylor, A.O. Barden, J.A. Brozik, Single-protein tracking reveals that NADPH mediates the insertion of cytochrome P450 reductase into a biomimetic of the endoplasmic reticulum, *J.*

- Am. Chem. Soc. 139 (2017) 5420–5430. <https://doi.org/10.1021/jacs.7b00663>.
- [48] W.C. Huang, J. Ellis, P.C.E. Moody, E.L. Raven, G.C.K. Roberts, Redox-linked domain movements in the catalytic cycle of cytochrome P450 reductase, *Structure*. 21 (2013) 1581–1589. <https://doi.org/10.1016/j.str.2013.06.022>.
- [49] M.J.I. Paine, N.S. Scrutton, A.W. Munro, A. Gutierrez, G.C.K. Roberts, C. Roland Wolf, Electron transfer partners of cytochrome P450. In P.R. Ortiz de Montellano (Ed.), *Cytochrome P450: Structure, Function, and Biochemistry*, Kluwer Academic / Plenum Publishers, New York, 2005, pp. 115–148,
- [50] B. Louerat-Oriou, A. Perret, D. Pompon, Differential redox and electron-transfer properties of purified yeast, plant and human NADPH-cytochrome P-450 reductases highly modulate cytochrome P-450 activities, *Eur. J. Biochem.* 258 (1998) 1040–1049. <https://doi.org/10.1046/j.1432-1327.1998.2581040.x>.
- [51] T. Abraham, R.N.A.H. Lewis, R.S. Hodges, R.N. McElhaney, Isothermal titration calorimetry studies of the binding of a rationally designed analogue of the antimicrobial peptide gramicidin s to phospholipid bilayer membranes, *Biochemistry*. 44 (2005) 2103–2112. <https://doi.org/10.1021/bi048077d>.
- [52] E.O. Yablokov, T.A. Sushko, P.V. Ershov, A.V. Florinskaya, O.V. Gnedenko, T.V. Shkel, I.P. Grabovec, N.V. Strushkevich, L.A. Kaluzhskiy, S.A. Usanov, A.A. Gilep, A.S. Ivanov, A large-scale comparative analysis of affinity, thermodynamics and functional characteristics of interactions of twelve cytochrome P450 isoforms and their redox partners, *Biochimie*. 162 (2019) 156–166. <https://doi.org/10.1016/j.biochi.2019.04.020>.
- [53] I. Ritacco, A. Saltalamacchia, A. Spinello, E. Ippoliti, A. Magistrato, All-atom simulations disclose how cytochrome reductase reshapes the substrate access/egress routes of its partner CYP450s, *J. Phys. Chem. Lett.* 11 (2020) 1189–1193. <https://doi.org/10.1021/acs.jpcclett.9b03798>.
- [54] G.F. Cawley, C.J. Batie, W.L. Backes, Substrate-dependent competition of

different P 450 isoenzymes for limiting NADPH-cytochrome P 450 reductase, Biochemistry. 34 (1995) 1244–1247. <https://doi.org/10.1021/bi00004a018>.

## Tables

**Table 1. Binding rates and dissociation constants of aromatase for the substrate androstenedione.**

Aro: CPR	K <sub>D</sub> <sup>a</sup> (μM)	k <sub>1</sub> (s <sup>-1</sup> )	k <sub>on</sub> (M <sup>-1</sup> s <sup>-1</sup> )	k <sub>off</sub> (s <sup>-1</sup> )	K <sub>D</sub> <sup>b</sup> (μM)
1: 0	0.98 ± 0.11	15.4 ± 0.8	5.1 ± 0.3 × 10 <sup>5</sup>	0.17 ± 0.06	0.33 ± 0.13
1: 3	0.72 ± 0.11	20.2 ± 0.9	7.0 ± 0.2 × 10 <sup>5</sup>	0.24 ± 0.05	0.34 ± 0.06

<sup>a</sup> K<sub>D</sub> values calculated from spectral equilibrium binding titrations.

<sup>b</sup> K<sub>D</sub> values calculated from these kinetic constants ( $k_{\text{off}}/k_{\text{on}}$ ).



**Table 2 Thermodynamic parameters measured from ITC experiments.**

<b>Combinations</b>	<b>K<sub>D</sub> (μM)</b>	<b>ΔH (kcal mol<sup>-1</sup>)</b>	<b>ΔG (kcal mol<sup>-1</sup>)</b>	<b>-TΔS (kcal mol<sup>-1</sup>)</b>
CPR <sub>sq</sub> /Aro - substrate	5.4 ± 1.2	9.5 ± 0.4	-7.2 ± 1.6	-16.7 ± 1.6
CPR <sub>sq</sub> /Aro + substrate	24.2 ± 6.9	6.0 ± 0.2	-6.3 ± 1.4	-12.3 ± 1.4

## Figure legends

**Scheme 1. Models for enzyme-substrate binding in human aromatase and role of cytochrome P450 reductase (CPR).** (A) In the induced fit model, the substrate binds the enzyme and induces a conformational rearrangement that optimizes the substrate-enzyme interaction. In a next step, CPR binds the enzyme-substrate complex and has no role in substrate binding. (B) In the conformational selection model, the enzyme shifts between different conformational states. The binding of CPR favors the enzyme conformation that is optimal for substrate binding that occurs in a next step.

**Figure 1. Substrate binding monitored by stopped-flow analysis.** (A) Difference spectra observed after mixing 1  $\mu$ M Aro with 10  $\mu$ M androstenedione in the stopped-flow apparatus. (B) Difference spectra observed after mixing 1  $\mu$ M Aro and 3  $\mu$ M CPR with 10  $\mu$ M androstenedione. The traces shown were collected after 0, 0.1, 0.2, 0.3, 0.4 and 0.5 seconds from mixing.

**Figure 2. Plot of the amount of spin shift as a function of the substrate concentration.** Black circles represent the amount of spin shift obtained from 1  $\mu$ M Aro in the absence of CPR; empty circles represent the amount of spin shift obtained from 1  $\mu$ M Aro pre-mixed with 3  $\mu$ M CPR (Aro:CPR = 1:3).

**Figure 3. Kinetics of substrate binding to aromatase.** (A) Kinetic traces ( $\Delta A_{394}$ ) obtained after mixing different amounts of the substrate androstenedione (0.25, 0.5, 1, 3, 6, 10, 20, 30  $\mu$ M) with 1  $\mu$ M Aro. (B) Kinetic traces ( $\Delta A_{394}$ ) obtained after mixing different amounts of the substrate (0.25, 0.5, 1, 3, 6, 10, 20, 30  $\mu$ M) with 1  $\mu$ M Aro and 3  $\mu$ M CPR (Aro:CPR = 1:3). All curves are fitted to single exponential functions.

**Figure 4. Analysis of the substrate binding rates.** (A) Plot of the binding rates as a function of substrate concentration with a fixed aromatase amount (1  $\mu$ M) in the absence (solid symbols) and presence (white symbols) of 3  $\mu$ M CPR (Aro:CPR = 1:3). (B) Plot of the binding rates as a function of aromatase concentration with a fixed substrate amount (2  $\mu$ M).

**Figure 5. UV-vs spectra of the protein samples used for ITC measurement.** (A) Spectra of 10  $\mu$ M CPR in potassium phosphate buffer (100 mM KPi, 10% glycerol, pH 7.0). (B) Aromatase spectra in the substrate-free form (black line) and upon incubation with the substrate androstenedione (gray line).

**Figure 6. Isothermal titration calorimetry traces for CPR<sub>sq</sub>-Aro complex formation.** ITC traces were obtained titrating CPR<sub>sq</sub> in the (A) substrate-free and (B) substrate-bound Aro in 100 mM KPi, 10% glycerol pH 7.0. The top panels show the raw data, the lower panels show the enthalpy changes plotted as a function of the CPR<sub>sq</sub>: Aro molar ratio. The black curves indicate the best fit to a single site model, the red circles represent the control experiments, where CPR<sub>sq</sub> was titrated into the ITC only containing buffer.